Conductivity and transparency of TiO_2 from first principles

André Schleife[1], Joel B. Varley[1,2], Anderson Janotti[2], and Chris G. Van de Walle[2]

[1]Condensed Matter and Materials Division, Lawrence Livermore National Laboratory, Livermore, California 94550, USA

[2]Materials Department, University of California, Santa Barbara, California 93106-5050, USA

ABSTRACT

Titanium dioxide is a versatile material with ubiquitous applications, many of which are critically linked to either light absorption or transparency in the visible spectral range in addition to electrical conductivity. Doping is a well-known way to influence those properties in order to bring them into a desired range. Working towards a comprehensive understanding of the electronic and optical properties of TiO_2 (as well as of the link between them) we review and summarize electronic-structure results that we obtained using cutting-edge theoretical spectroscopy techniques. We focus on the formation of electron and hole polarons and we elucidate the influence of doping on the optical properties of TiO_2. In addition, we present new results for the reflectivity of pure TiO_2.

Keywords: titania, first principles, electron polaron, hole polaron, doping, reflectivity, optical absorption

1. INTRODUCTION

Oxide semiconductors currently attract a lot of attention due to various existing and potential applications: with their large band gap and high (mostly n-type) dopability they form the class of transparent conducting oxides (TCOs) and are interesting for optoelectronics,[1] photovoltaics,[2] and other transparent electronics[3] devices. In addition, oxide materials have great potential for photocatalysis[4] and water splitting.[5]

Titanium dioxide, TiO_2, is an oxide semiconductor that commonly appears either in rutile or anatase phase, both of which have large band gaps > 3 eV.[6,7,8,9] While a large (optical) gap fulfills merely the first of two requirements for TCO applications, it actually *hampers* photocatalytic activity because the amount of harvested light is extremely low. *Doping* offers a means of controlling the properties for both the TCO and photocatalysis applications. Depending on the dopants that are used they can provide free carriers to increase the conductivity of TiO_2 and enable applications in electronics.[10] Alternatively, dopants can introduce defect levels and break the crystal symmetry, which increases the absorption of visible light and paves the way for more efficient photocatalysis.

In order to achieve a thorough theoretical understanding of these aspects, our group has performed first-principles calculations for TiO_2, its defects, and different dopants.[11,12,13,14] Building on these results we investigated the formation of small polarons in the presence of free electrons (n-doping) or holes (that can be created in the photoabsorption processes).[15,16] Based on theoretical spectroscopy techniques we highlighted the influence of nitrogen (N_O) substitutionals as well as alloying with sulfur (S) on the optical absorption. In this work we summarize and discuss the key results. In addition, we briefly highlight the optical anisotropy of pure rutile TiO_2 based on new results for the reflectivity that we derive from the dielectric function in this work.

The theoretical and computational approaches are briefly outlined in Sec. 2. Formation of small electron and hole polarons in TiO_2 is discussed in Sec. 3 and the optical properties in the presence of N or S are explored in Sec. 4. Section 5 concludes the paper.

Further author information:
A. Schleife: E-mail: a.schleife@llnl.gov
J. B. Varley: E-mail: varley2@llnl.gov
A. Janotti: E-mail: janotti@engineering.ucsb.edu
C. G. Van de Walle: E-mail: vandewalle@mrl.ucsb.edu

Solar Hydrogen and Nanotechnology VIII, edited by Yosuke Kanai, David Prendergast, Proc. of SPIE Vol. 8822, 882205 · © 2013 SPIE
CCC code: 0277-786X/13/$18 · doi: 10.1117/12.2024566

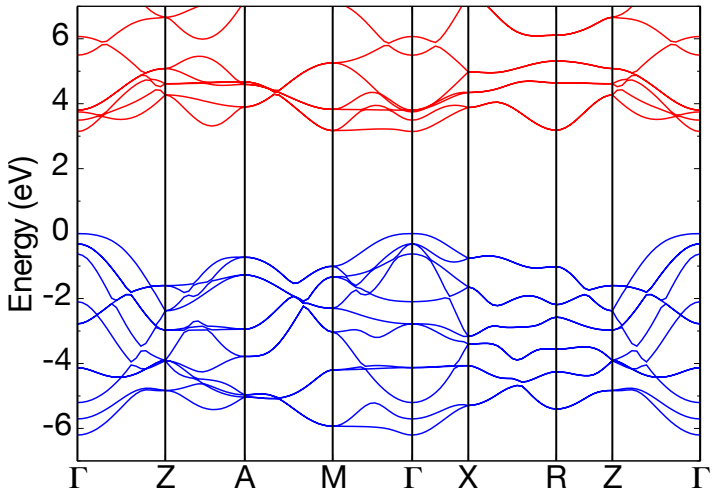

Figure 1. (Color online) Band structure of rutile TiO_2 calculated with the HSE06 screened hybrid functional. The upper valence bands are shown in blue and the conduction bands in red. The valence-band maximum is used as energy zero.

2. COMPUTATIONAL APPROACH

The results reviewed in this work are based on parameter-free electronic structure calculations that we performed for TiO_2 within generalized Kohn-Sham theory[17] as well as many-body perturbation theory. For an accurate description of TiO_2 we go beyond the local-density approximation[18,19,20] (LDA) for the exchange-correlation functional within density functional theory[18] (DFT): We use the non-local hybrid functional of Heyd, Scuseria, and Ernzerhof[21,22] (HSE06). In this approach the exchange-correlation potential is divided into long- and short-range parts using a range-separation parameter of $0.2\,\text{Å}^{-1}$. A fraction (α=0.25) of Hartree-Fock exchange is combined with the generalized-gradient approximation (GGA) [using the semi-local potential of Perdew, Burke, and Ernzerhof[23] (PBE)] for the short-range part. The correlation and the long-range part of the exchange potential are described by PBE as well.

The electron-ion interaction is described by means of the projector augmented-wave method[24] and we employ a cutoff of 400 eV for the plane-wave basis to study the electron and hole polarons. Supercells consisting of 216 atoms were used for rutile TiO_2 and the corresponding Brillouin zones were sampled by $2 \times 2 \times 2$ Monkhorst-Pack[25] $\mathbf{k}$ points (Γ only for the electron polaron) for the relaxation of the structures. Afterwards, total energies were evaluated using just the Γ point to obtain the correct occupation for free-electron or free-hole states. Spin polarization was included in our calculations and all calculations were carried out using the VASP code.[26,27]

Previous studies indicated that this approach provides lattice constants within 1 % of the experimental values as well as accurate results for the band gaps,[12,13] as seen in the calculated band structure in Fig. 1. The inclusion of Hartree-Fock exchange in the HSE functional mitigates the deficiencies of DFT-LDA/GGA for the description of the electronic structure, hence, we do not solve a quasiparticle equation but use the HSE electronic structure instead as an approximation to include quasiparticle effects.

In order to investigate the influence of dopants or alloying on the light absorption in the visible spectral range we pursued two different approaches: (i) We performed impurity calculations for supercells of 72 atoms (rutile phase) or 108 atoms (anatase phase) to compute the lowest optical absorption and emission energies in the presence of nitrogen-related defects.[12] (ii) We computed the dielectric function for rutile $TiO_{2(1-x)}S_{2x}$ alloys with compositions between 0 and 0.25 using supercells of 12 to 96 atoms.[11]

For different oxides[28,29] and their alloys[30] it has been shown before that it is important to include excitonic and local-field effects for a correct description of dielectric functions or optical absorption spectra; this goes beyond the framework outlined above. We solved the Bethe-Salpeter equation (BSE) for the optical polarization function P[31,32] based on a DFT-LDA[33] electronic structure.[14] Optical transition matrix elements are calculated using the longitudinal approximation.[34] This allows us to compute the macroscopic dielectric function in the optical limit of vanishing photon wave vector. In order to keep the calculations tractable we again avoided the quasiparticle approach, which becomes very expensive for

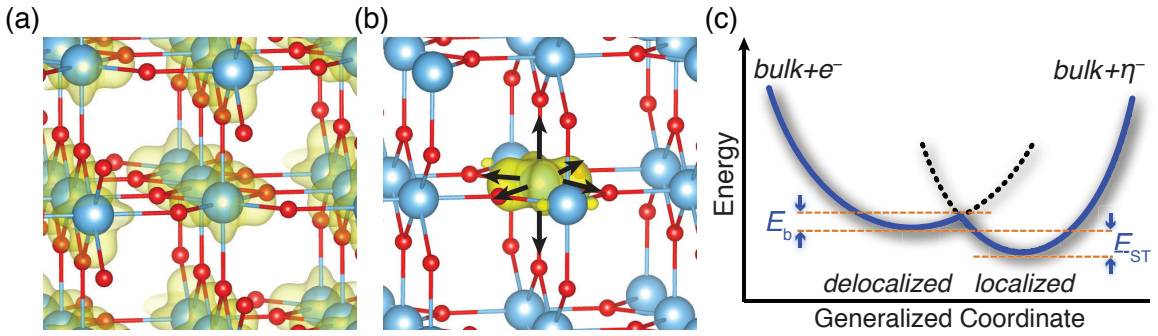

Figure 2. (Color online) Schematic isosurface (10 % of the maximum value) plot of charge density associated with (a) a free (delocalized) electron and (b) a (localized) self-trapped electron polaron. Ti atoms are shown as blue (large) circles and oxygen atoms as red (small) circles. The schematic configuration coordinate diagram (c) shows energy as a function of the lattice distortion for a free electron (e^-) and a localized electron (ξ^-).

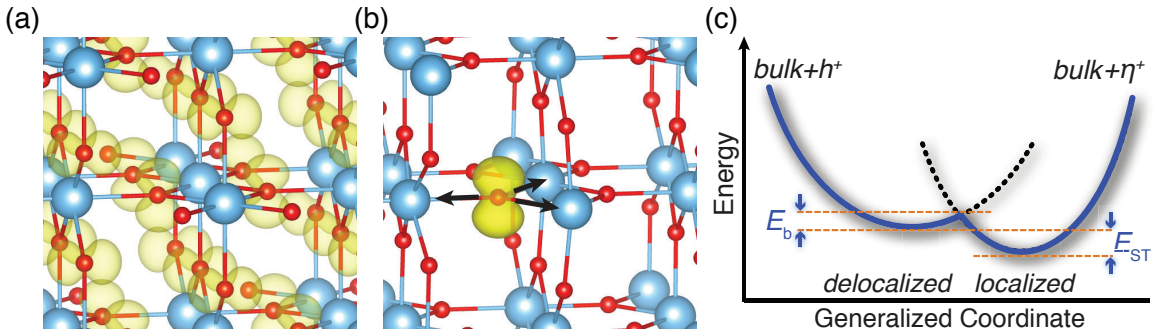

Figure 3. (Color online) Schematic isosurface (10 % of the maximum value) plot of charge density associated with (a) a free (delocalized) hole and (b) a (localized) self-trapped hole polaron. Ti atoms are shown as blue (large) circles and oxygen atoms as red (small) circles. The schematic configuration coordinate diagram (c) shows energy as a function of the lattice distortion for a free hole (h^+) and a localized hole (η^+).

large supercells. We used **k**-point meshes dense enough for calculating optical spectra, i.e., maximum **k**-point distances of 0.36 Å^{-1} (see Refs. 11 and 14 for details).

3. BEHAVIOR OF EXCESS ELECTRONS AND HOLES

When electrons or holes are created through doping or photoexcitation, they may remain delocalized [cf. Figs. 2(a) and 3(a)] or become localized [cf. Figs. 2(b) and 3(b)]. A thorough understanding of this potential localization is important since it critically impacts conductivity. In the case of n-type TiO_2 both high mobilities[35] as well as formation of (localized) small polarons[36] have been reported. Many TCOs can be easily n-doped, however, it would be highly beneficial to achieve p doping in one and the same material. Since the valence bands are derived from relatively localized O $2p$ states and exhibit large effective masses, again the possibility of polaron formation arises.[37]

In order to investigate the formation of small electron (hole) polarons we add (remove) one electron to the conduction-band minimum (from the valence-band maximum) in a supercell. The lattice is relaxed after introducing small random displacements of atoms. In Figs. 2 and 3 the respective charge distributions of the localized and the delocalized configuration are shown. The stability of the self-trapped electron (hole) configuration ξ^- (η^+) with respect to the delocalized carrier e^- (h^+) in an unperturbed crystal can be analyzed using the self-trapping energy E_{ST},

$$E_{\mathrm{ST}} = E_{\mathrm{tot}}[X_m O_n : e^-/h^+] - E_{\mathrm{tot}}[X_m O_n : \xi^-/\eta^+] - \Delta\bar{V}, \tag{1}$$

with $E_{\rm tot}[X_mO_n : e^-/h^+]$ being the total energy of an unperturbed supercell containing an additional electron (hole), $E_{\rm tot}[X_mO_n : \xi^-/\eta^+]$ being the total energy of the relaxed cell containing the localized carrier, and $\Delta\bar{V}$ accounting for the alignment of the average electrostatic potentials of both cells.

Using this approach we found[15] that self-trapping (localization) of a delocalized electron in the conduction band leads to a slight energy gain of about $E_{\rm ST}$=0.15 eV (cf. Fig. 2). Hence, the formation of a small electron polaron is favorable in TiO_2. In addition, we computed a value for the migration barrier of these small polarons of about 0.03 eV. Although small electron polarons in rutile are more stable than delocalized electrons, Hall measurements[35] show high electron mobilities that cannot be attributed to hopping of small polarons. We attribute this to the existence of a barrier for a delocalized electron to convert to a small polaron. This barrier prevents electrons injected during transport measurements from becoming localized, so that Hall measurements probe mainly free, delocalized electrons. Optical spectroscopy measurements,[38] on the other hand, observe small polarons that have become stabilized. Self-trapped electrons in the form of small polarons have also been detected by electron paramagnetic resonance (EPR).[39,40,41,42]

For the self-trapped hole state (cf. Fig. 3) we found a localized wave function that resembles an O $2p$ orbital and is mainly localized on one oxygen atom, with a significant extension of the surrounding Ti-O bonds.[16] With $E_{\rm ST}$=0.11 eV the self-trapping energy is slightly smaller than in the case of the electron polaron and we compute a larger migration barrier of 0.11 eV. Self-trapped holes have also been found in EPR experiments in rutile TiO_2 when subjected to 2.81 eV He-Cd laser illumination at low temperatures.[39,40] For both self-trapped holes and electrons, extended and point defects, such as surfaces, vacancies,[41] and impurities,[41,43,44] can result in more stable trapping sites.

Optical excitation with sufficiently energetic light can create electron-hole pairs that lead to self-trapped excitons. The EPR experiments illustrate that excitation with below-band-gap light can also lead to self-trapped electrons or holes.[39] In the case of hole polarons, an electron from the valence band may be excited to an unoccupied defect-related state within the gap, leaving a hole that can self-trap at low temperatures. Similarly, an electron can be promoted to the conduction-band minimum from an occupied defect state within the band gap, and may subsequently self-trap. Regardless of how the holes in the valence band are created, small hole polarons may recombine with free electrons in the conduction band, resulting in a luminescence band at energies significantly smaller than the band gap. In rutile, we predicted a broad emission peak to occur at 2.04 eV for isolated small hole polarons that recombine with free electrons in this manner.[16] In an analogous process, electron polarons may recombine with free holes in the valence band, which we find leads to a broad luminescence peak at 2.50 eV. Therefore for excitations that generate electron-hole pairs, both types of luminescence peaks may be observed at temperatures low enough to allow for self-trapping. Such recombination events may account for the green luminescence in Al-doped rutile excited with ultraviolet light at low temperatures.[44]

4. ABSORPTION IN THE VISIBLE SPECTRAL RANGE

4.1 The role of nitrogen doping

The incorporation of N has been shown to enhance visible-light absorption, leading to improved photochemical activity.[45,46,47,48,49] Despite the abundance of literature on N in TiO_2,[45,50,51,52] a number of the reports were conflicting and the fundamental mechanisms underlying the behavior of N remained largely unresolved. It has been generally accepted that transitions from N-related states in the band gap lead to visible-light absorption; questions such as whether the N atoms predominantly incorporate at interstitial sites or on substitutional O sites (N_O), and whether the behavior of N in rutile is different from that in anatase, were still unanswered. Here we describe our recent work to evaluate the stability of the relevant N-related defects in both polymorphs,[12] finding that impurity-band transitions from N_O are the origin of the lower absorption threshold in N-doped titania.

The initial experimental work established the correlation between N incorporation and visible-light absorption and photocatalytic activity via x-ray photoelectron spectroscopy measurements.[45] Since then, two main peaks attributed to the N $1s$ state have been correlated with photocatalytic activity, one existing at $\sim$396 eV and the other at $\sim$400 eV.[45,51,52,53] While the $\sim$396 eV was identified as N_O in molecular-beam-epitaxy grown anatase,[53] different groups have suggested alternative explanations for the peaks, with N_O, interstitial NO, and N-H complexes as proposed sources.[45,51,52,54] Without an experimental consensus of the species responsible for the peaks, the nature of the N-related defect(s) associated with visible-light absorption has remained ambiguous.

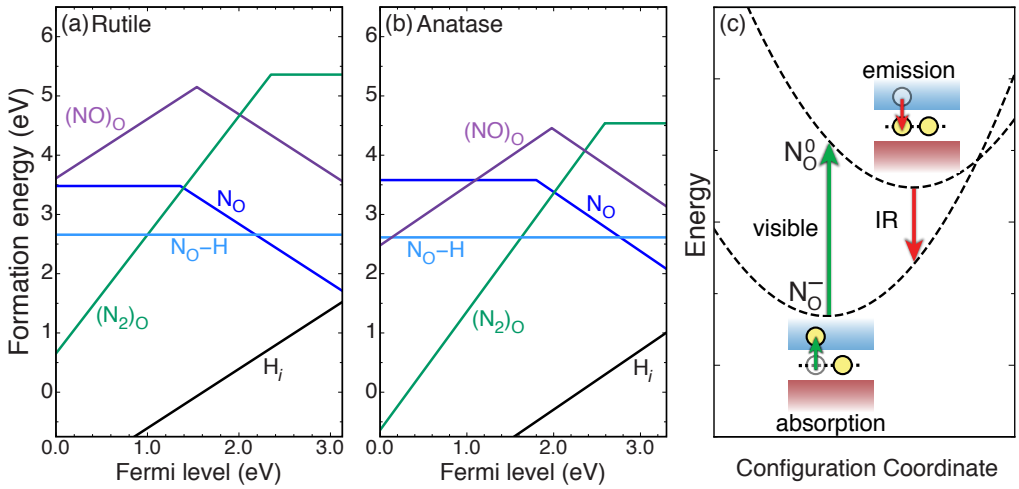

Figure 4. (Color online) Formation energy diagram for N-related defects in (a) rutile and (b) anatase phases of TiO_2. Configuration coordinate diagram (c) for N-related defects in TiO_2. Adapted from J. B. Varley, A. Janotti, and C. G. Van de Walle, Adv. Mater. **23**, 2343 (2011).

Previous computations have further complicated the picture, predicting that N_O leads to the observed red-shift in anatase, but would result in a blue-shift in rutile,[55] an observation not compatible with recent experiments on single crystals.[47,48] Subsequent theoretical reports suggested that in addition to substitutional N_O, N as an interstitial[56] and as a complex with O vacancies (V_O)[57] could also play a role in visible-light absorption.

These unresolved issues regarding visible light absorption in TiO_2 motivated us to investigate the role of N impurities in bulk rutile and anatase using the advanced first-principles calculations outlined in Sec. 2.[12] We focused on two aspects of nitrogen doping that could resolve the discrepancies in the literature: (i) how N affects the electrical and optical properties of TiO_2, and (ii) possible sources that could compensate effects of N incorporation. For the former, we calculated formation energies for substitutional and interstitial configurations of N impurities in TiO_2, and analyzed their thermodynamic and optical transition levels. For the latter, we focused on the interaction of N with H, a ubiquitous impurity that is likely to be incorporated along with N in N-doped TiO_2, since H is present in common precursors such as NH_3.

Our key conclusions are summarized in Fig. 4. In Fig. 4(a) and (b) we plot the formation energies of N-related defects, where it can be seen that N prefers to occupy the O site in n-type TiO_2, as opposed to interstitial sites such as $(NO)_O$ or $(N_2)_O$. Qualitatively, it can be seen that N behaves similarly in rutile and anatase in terms of the electronic transition levels. The calculated optical transitions [cf. Fig. 4(c)] for $N_O^- + \hbar\omega \rightarrow N_O^0 + e^-$ are also similar in both polymorphs, and result in a defect-mediated absorption onset in the visible range, in good agreement with experimental observations. Finally, from Fig. 4 it can also be seen that H bonds to N_O, forming stable N-H complexes with significant binding energies.[12] The hybridization between the H_i and N_O states removes the N_O impurity state from the band gap, thereby eliminating the advantageous effects of N in enhancing visible-light absorption and reducing the amount of nitrogen that N contributes to the photocatalytic activity.

4.2 Effects of sulfur alloying

As outlined above, it is a central goal to modify TiO_2 such that a larger part of the solar spectrum can be harvested for photochemical applications. Many efforts were undertaken to extend the optical absorption into the visible spectral range. Both experimental as well as theoretical studies investigated doping, e.g., with N, F, C, Se, P, or S.[12,14,45,47,58,59,60,60,61,62] In addition, co-doping[60,62] and the engineering of disordered phases[63,64] were also explored.

We computed the optical absorption properties (including excitonic and local-field effects) of $TiO_{2(1-x)}S_{2x}$ alloys with varying composition, using the techniques outlined in Sec. 2.[11] In Fig. 5(a) these results are illustrated for the dielectric function in the vicinity of the absorption edge. Since optical transitions from the uppermost valence states into the lowest conduction states are forbidden by dipole selection rules, the first strong absorption peak in pure rutile TiO_2 only occurs at

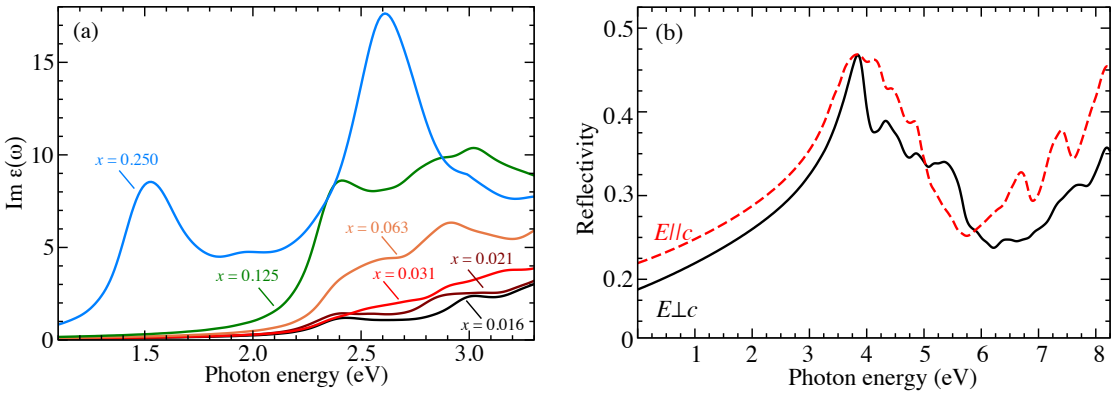

Figure 5. (Color online) Imaginary part of the dielectric function averaged over all polarization directions (a) of $TiO_{2(1-x)}S_{2x}$ for different compositions x. In (b) the reflectivity of pure rutile TiO_2 is shown for $E \perp c$ (solid black) and $E||c$ (dashed red).

about 4.0 eV. Consequently, all the peaks visible in Fig. 5(a) arise exclusively from S doping. This shows that even a very small S concentration in the alloy of about 1.5 % is enough to significantly increase the absorption in the visible spectral range.

We found that two effects contribute: (i) Replacing one oxygen atom by an S atom leads to defect levels in the band gap and optical transitions from these defect levels into the lowest conduction-band states have large oscillator strengths. (ii) In addition, the alloy no longer has ideal rutile lattice symmetry; this causes transitions from TiO_2 valence states into the conduction band to also acquire appreciable oscillator strength. The latter effect is the reason for increased optical absorption in the near-ultraviolet spectral region and occurs for all the different S concentrations that we investigated. We speculate that the small perturbations of the ideal rutile lattice that inevitably occur in real samples have a similar impact and contribute to the usefulness of TiO_2 as a photocatalyst, in spite of its fundamental gap being dipole-forbidden.

We have also used our results for the dielectric function of pure rutile TiO_2 to study the optical anisotropy. By means of the relation

$$R(\omega) = \left| \frac{\sqrt{\varepsilon(\omega)} - 1}{\sqrt{\varepsilon(\omega)} + 1} \right|^2 \tag{2}$$

we compute the reflectivity from the dielectric function. The results are shown in Fig. 5(b). For both polarization directions there is a broad peak feature (with a reflectivity of almost 50 %) centered around 4 eV. The reflectivity in the visible spectral range is less than half as large as around the maximum of the peak. Except in a narrow range between 5 and 6 eV, the reflectivity for extraordinary ($E||c$) is higher than for ordinary light polarization.

5. SUMMARY AND OUTLOOK

We reviewed some of our earlier work on electronic structure calculations for rutile and anatase TiO_2. We reported that both electrons and holes in rutile TiO_2 show a tendency to localize and form small polarons. This seems to be a common phenomenon in many oxides, with important consequences for applications, hence it deserves further theoretical as well as experimental attention. Theoretical approaches that are capable of accurately describing the physics of localized states and excited electronic states remain a challenge, in particular for complex materials, due to their large computational cost. At the same time, additional experiments are called for to study carrier and polaron mobilities as well as the barriers that separate localized and delocalized configurations.

To explore pathways to increase absorption of visible light for photocatalysis, we discussed our work on the influence of nitrogen and sulfur doping and also reported new results for the reflectivity of undoped rutile TiO_2. We showed that both the defect-induced states themselves as well as the modified crystal symmetry contribute to increased absorption. Future work should address identifying dopants that not only efficiently increase the absorption of visible light, but also facilitate spatial separation of electron-hole pairs created in the optical absorption process. Joint experimental and theoretical efforts will be required to address this important issue.

Acknowledgments

Fruitful collaborations with P. Moses, P. Rinke, D. Steiauf, and N. Umezawa are gratefully acknowledged. JV was supported by the NSF MRSEC Program (DMR-1121053). AJ and CVdW were supported by the U.S. Army Research Office (W911-NF-11-1-0232). Computational resources were provided by the Center for Scientific Computing at the CNSI and MRL (an NSF MRSEC, DMR-1121053) (NSF CNS-0960316), and by the Extreme Science and Engineering Discovery Environment (XSEDE), supported by NSF (OCI-1053575 and DMR07-0072N). Part of this work was performed under the auspices of the U.S. Department of Energy at Lawrence Livermore National Laboratory under Contract DE-AC52-07A27344.

REFERENCES

[1] Ginley, D. S. and Bright, C., "Transparent conducting oxides," *MRS Bull.* **25**, 15–18 (2000).

[2] Fortunato, E., Ginley, D., Hosono, H., and Paine, D. C., "Transparent conducting oxides for photovoltaics," *MRS Bull.* **32**, 242–247 (2007).

[3] Ramirez, A. P., "Oxide electronics emerge," *Science* **315**, 1377–1378 (2007).

[4] O'Regan, B. and Grätzel, M., "A low-cost, high-efficiency solar cell based on dye-sensitized colloidal TiO_2 films," *Nature* **353**, 737–740 (1991).

[5] Fujishima, A. and Honda, K., "Electrochemical photolysis of water at a semiconductor electrode," *Nature* **238**, 37–38 (1972).

[6] Diebold, U., "The surface science of titanium dioxide," *Surf. Sci. Rep.* **48**, 53–229 (2003).

[7] Pascual, J., Camassel, J., and Mathieu, H., "Fine structure in the intrinsic absorption edge of TiO_2," *Phys. Rev. B* **18**, 5606–5614 (1978).

[8] Tang, H., Berger, H., Schmid, P., Lvy, F., and Burri, G., "Photoluminescence in TiO_2 anatase single crystals," *Solid State Commun.* **87**, 847–850 (1993).

[9] Kavan, L., Grätzel, M., Gilbert, S. E., Klemenz, C., and Scheel, H. J., "Electrochemical and photoelectrochemical investigation of single-crystal anatase," *J. Am. Chem. Soc.* **118**, 6716–6723 (1996).

[10] Chen, D., Xu, G., Miao, L., Chen, L., Nakao, S., and Jin, P., "W-doped anatase TiO_2 transparent conductive oxide films: Theory and experiment," *J. Appl. Phys.* **107**, 063707 (2010).

[11] Schleife, A., Rinke, P., Bechstedt, F., and Van de Walle, C. G., "Enhanced optical absorption due to symmetry breaking in $TiO_{2(1-x)}S_{2x}$ alloys," *J. Phys. Chem. C* **117**, 4189–4193 (2013).

[12] Varley, J. B., Janotti, A., and Van de Walle, C. G., "Mechanism of visible-light photocatalysis in nitrogen-doped TiO_2," *Adv. Mater.* **23**, 2343–2347 (2011).

[13] Janotti, A., Varley, J. B., Rinke, P., Umezawa, N., Kresse, G., and Van de Walle, C. G., "Hybrid functional studies of the oxygen vacancy in TiO_2," *Phys. Rev. B* **81**, 085212 (2010).

[14] Umezawa, N., Janotti, A., Rinke, P., Chikyow, T., and Van de Walle, C. G., "Optimizing optical absorption of TiO_2 by alloying with TiS_2," *Appl. Phys. Lett.* **92**, 041104 (2008).

[15] Janotti, A., Franchini, C., Varley, J. B., Kresse, G., and Van de Walle, C. G., "Dual behavior of excess electrons in rutile TiO_2," *Phys. Status Solidi-R* **7**, 199–203 (2013).

[16] Varley, J. B., Janotti, A., Franchini, C., and Van de Walle, C. G., "Role of self-trapping in luminescence and p-type conductivity of wide-band-gap oxides," *Phys. Rev. B* **85**, 081109 (2012).

[17] Seidl, A., Görling, A., Vogl, P., Majewski, J. A., and Levy, M., "Generalized Kohn-Sham schemes and the band-gap problem," *Phys. Rev. B* **53**, 3764–3774 (1996).

[18] Kohn, W. and Sham, L. J., "Self-consistent equations including exchange and correlation effects," *Phys. Rev.* **140**, A1133–A1138 (1965).

[19] Hohenberg, P. and Kohn, W., "Inhomogeneous electron gas," *Phys. Rev.* **136**, B864–B871 (1964).

[20] Ceperley, D. M. and Alder, B. J., "Ground state of the electron gas by a stochastic method," *Phys. Rev. Lett.* **45**, 566–569 (1980).

[21] Heyd, J., Scuseria, G. E., and Ernzerhof, M., "Hybrid functionals based on a screened Coulomb potential," *J. Chem. Phys.* **118**, 8207–8215 (2003).

[22] Heyd, J., Scuseria, G. E., and Ernzerhof, M., "Erratum: "Hybrid functionals based on a screened Coulomb potential" [J. Chem. Phys. **118**, 8207 (2003)]," *J. Chem. Phys.* **124**, 219906 (2006).

[23] Perdew, J. P., Burke, K., and Ernzerhof, M., "Generalized gradient approximation made simple," *Phys. Rev. Lett.* **77**, 3865–3868 (1996).
[24] Blöchl, P. E., "Projector augmented-wave method," *Phys. Rev. B* **50**, 17953–17979 (1994).
[25] Monkhorst, H. J. and Pack, J. D., "Special points for Brillouin-zone integrations," *Phys. Rev. B* **13**, 5188–5192 (1976).
[26] Kresse, G. and Furthmüller, J., "Efficiency of ab-initio total energy calculations for metals and semiconductors using a plane-wave basis set," *Comp. Mater. Sci.* **6**, 15–50 (1996).
[27] Kresse, G. and Joubert, D., "From ultrasoft pseudopotentials to the projector augmented-wave method," *Phys. Rev. B* **59**, 1758–1775 (1999).
[28] Schleife, A., Rödl, C., Fuchs, F., Furthmüller, J., and Bechstedt, F., "Optical and energy-loss spectra of MgO, ZnO, and CdO from ab initio many-body calculations," *Phys. Rev. B* **80**, 035112 (2009).
[29] Schleife, A., Varley, J. B., Fuchs, F., Rödl, C., Bechstedt, F., Rinke, P., Janotti, A., and Van de Walle, C. G., "Tin dioxide from first principles: Quasiparticle electronic states and optical properties," *Phys. Rev. B* **83**, 035116 (2011).
[30] Schleife, A., Rödl, C., Furthmüller, J., and Bechstedt, F., "Electronic and optical properties of $Mg_xZn_{1-x}O$ and $Cd_xZn_{1-x}O$ from ab initio calculations," *New J. Phys.* **13**, 085012 (2011).
[31] Onida, G., Reining, L., and Rubio, A., "Electronic excitations: density-functional versus many-body Green's-function approaches," *Rev. Mod. Phys.* **74**, 601–659 (2002).
[32] Rödl, C., Fuchs, F., Furthmüller, J., and Bechstedt, F., "Ab initio theory of excitons and optical properties for spin-polarized systems: Application to antiferromagnetic MnO," *Phys. Rev. B* **77**, 184408 (2008).
[33] Perdew, J. P. and Zunger, A., "Self-interaction correction to density-functional approximations for many-electron systems," *Phys. Rev. B* **23**, 5048–5079 (1981).
[34] Gajdoš, M., Hummer, K., Kresse, G., Furthmüller, J., and Bechstedt, F., "Linear optical properties in the projector-augmented wave methodology," *Phys. Rev. B* **73**, 045112 (2006).
[35] Yagi, E., Hasiguti, R. R., and Aono, M., "Electronic conduction above 4 K of slightly reduced oxygen-deficient rutile TiO_{2-x}," *Phys. Rev. B* **54**, 7945–7956 (1996).
[36] Austin, I. G. and Mott, N. F., "Polarons in crystalline and non-crystalline materials," *Adv. Phys.* **50**, 757–812 (2001).
[37] Stoneham, A. M., Gavartin, J., Shluger, A. L., Kimmel, A. V., Ramo, D. M., Rønnow, H. M., Aeppli, G., and Renner, C., "Trapping, self-trapping and the polaron family," *J. Phys. Condens. Mat.* **19**, 255208 (2007).
[38] Bogomolov, V. N. and Mirlin, D. N., "Optical absorption by polarons in rutile (TiO_2) single crystals," *Phys. Status Solidi B* **27**, 443–453 (1968).
[39] Yang, S., Halliburton, L. E., Manivannan, A., Bunton, P. H., Baker, D. B., Klemm, M., Horn, S., and Fujishima, A., "Photoinduced electron paramagnetic resonance study of electron traps in TiO_2 crystals: Oxygen vacancies and Ti^{3+} ions," *Appl. Phys. Lett.* **94**, 162114 (2009).
[40] Yang, S., Brant, A. T., and Halliburton, L. E., "Photoinduced self-trapped hole center in TiO_2 crystals," *Phys. Rev. B* **82**, 035209 (2010).
[41] Yang, S. and Halliburton, L. E., "Fluorine donors and Ti^{3+} ions in TiO_2 crystals," *Phys. Rev. B* **81**, 035204 (2010).
[42] Yang, S., Brant, A. T., Giles, N. C., and Halliburton, L. E., "Intrinsic small polarons in rutile TiO_2," *Phys. Rev. B* **87**, 125201 (2013).
[43] Brant, A. T., Yang, S., Giles, N. C., and Halliburton, L. E., "Hydrogen donors and Ti^{3+} ions in reduced TiO_2 crystals," *J. Appl. Phys.* **110**, 053714 (2011).
[44] Zwingel, D., "The structure of trapped hole centres in Al-doped TiO_2," *Solid State Comm.* **20**, 397–400 (1976).
[45] Asahi, R., Morikawa, T., Ohwaki, T., Aoki, K., and Taga, Y., "Visible-light photocatalysis in nitrogen-doped titanium oxides," *Science* **293**, 269–271 (2001).
[46] Kobayakawa, K., Murakami, Y., and Sato, Y., "Visible-light active N-doped TiO_2 prepared by heating of titanium hydroxide and urea," *J. Photochem. Photobiol., A* **170**, 177–179 (2005).
[47] Chambers, S. A., Cheung, S. H., Shutthanandan, V., Thevuthasan, S., Bowman, M. K., and Joly, A. G., "Properties of structurally excellent N-doped TiO_2 rutile," *Chem. Phys* **339**, 27–35 (2007).
[48] Cheung, S. H., Nachimuthu, P., Joly, A. G., Engelhard, M. H., Bowman, M. K., and Chambers, S. A., "N incorporation and electronic structure in N-doped TiO_2(110) rutile," *Surf. Sci.* **601**, 1754–1762 (2007).
[49] Cheung, S. H., Nachimuthu, P., Engelhard, M. H., Wang, C. M., and Chambers, S. A., "N incorporation, composition and electronic structure in N-doped TiO_2(001) anatase epitaxial films grown on $LaAlO_3$(001)," *Surf. Sci.* **602**, 133–141 (2008).

[50] Irie, H., Watanabe, Y., and Hashimoto, K., "Nitrogen-concentration dependence on photocatalytic activity of $TiO_{2-x}N_x$ powders," *J. Phys. Chem. B* **107**, 5483–5486 (2003).

[51] Diwald, O., Thompson, T. L., Zubkov, T., , Walck, S. D., and Yates, J. T., "Photochemical activity of nitrogen-doped rutile TiO_2(110) in visible light," *J. Phys. Chem. B* **108**, 6004–6008 (2004).

[52] Chen, X. and Burda, C., "Photoelectron spectroscopic investigation of nitrogen-doped titania nanoparticles," *J. Phys. Chem. B* **108**, 15446–15449 (2004).

[53] Ohsawa, T., Lyubinetsky, I., Du, Y., Henderson, M. A., Shutthanandan, V., and Chambers, S. A., "Crystallographic dependence of visible-light photoactivity in epitaxial $TiO_{2-x}N_x$ anatase and rutile," *Phys. Rev. B* **79**, 085401 (2009).

[54] Asahi, R. and Morikawa, T., "Nitrogen complex species and its chemical nature in TiO_2 for visible-light sensitized photocatalysis," *Chem. Phys* **339**, 57–63 (2007).

[55] Di Valentin, C., Pacchioni, G., and Selloni, A., "Origin of the different photoactivity of N-doped anatase and rutile TiO_2," *Phys. Rev. B* **70**, 085116 (2004).

[56] Valentin, C. D., Finazzi, E., Pacchioni, G., Selloni, A., Livraghi, S., Paganini, M. C., and Giamello, E., "N-doped TiO_2: Theory and experiment," *Chem. Phys* **339**, 44–56 (2007).

[57] Rumaiz, A. K., Woicik, J. C., Cockayne, E., Lin, H. Y., Jaffari, G. H., and Shah, S. I., "Oxygen vacancies in N doped anatase TiO_2: Experiment and first-principles calculations," *Appl. Phys. Lett.* **95**, 262111 (2009).

[58] Umebayashi, T., Yamaki, T., Itoh, H., and Asai, K., "Band gap narrowing of titanium dioxide by sulfur doping," *Appl. Phys. Lett.* **81**, 454–456 (2002).

[59] Li, H., Li, J., and Huo, Y., "Highly active TiO_2N photocatalysts prepared by treating TiO_2 precursors in NH_3/ethanol fluid under supercritical conditions," *J. Phys. Chem. B* **110**, 1559–1565 (2006).

[60] Sakai, Y. W., Obata, K., Hashimoto, K., and Irie, H., "Enhancement of visible light-induced hydrophilicity on nitrogen and sulfur-codoped TiO_2 thin films," *Vacuum* **83**, 683–687 (2008).

[61] Long, R. and English, N. J., "Synergistic effects of Bi/S codoping on visible light-activated anatase TiO_2 photocatalysts from first principles," *J. Phys. Chem. C* **113**, 8373–8377 (2009).

[62] Wang, P., Liu, Z., Lin, F., Zhou, G., Wu, J., Duan, W., Gu, B.-L., and Zhang, S. B., "Optimizing photoelectrochemical properties of TiO_2 by chemical codoping," *Phys. Rev. B* **82**, 193103 (2010).

[63] Chen, X., Liu, L., Yu, P. Y., and Mao, S. S., "Increasing solar absorption for photocatalysis with black hydrogenated titanium dioxide nanocrystals," *Science* **331**, 746–750 (2011).

[64] Hu, Y. H., "A highly efficient photocatalyst-hydrogenated black TiO_2 for the photocatalytic splitting of water," *Angew. Chem. Int. Edit.* **51**, 12410–12412 (2012).